Article

Electrostatic modulation of the electronic properties of Nb-doped $SrTiO_3$ superconducting films

TAKAHASHI, Kei, *et al*.

Abstract

We have performed ferroelectric field effect experiments using an epitaxialheterostructure composed of ferroelectricPb(Zr0.2Ti0.8)O3 and superconducting Nb-doped SrTiO3. The films were prepared on (001) SrTiO3 substrates by off-axis radio-frequency magnetron sputtering and pulsed-laser deposition. By switching the polarization field of the 500-Å-thick Pb(Zr0.2Ti0.8)O3 layer, a large change of about 30% in resistivity and a 20% shift of Tc (ΔTc~0.05K) were induced in the 400-Å-thick epitaxial Nb-doped SrTiO3 layer. The relationship between Tc and the electrostatically modulated average carrier concentration can be mapped onto the phase diagram of chemically doped SrTiO3

Reference

TAKAHASHI, Kei, *et al*. Electrostatic modulation of the electronic properties of Nb-doped $SrTiO_3$ superconducting films. *Applied physics letters*, 2004, vol. 84, no. 10, p. 1722

DOI : 10.1063/1.1667279

Electrostatic modulation of the electronic properties of Nb-doped $SrTiO_3$ superconducting films

K. S. Takahashi,[a] D. Matthey, D. Jaccard, and J.-M. Triscone
DPMC, University of Geneva, 24 Quai Ernest Ansermet, 1211 Geneva 4, Switzerland

K. Shibuya, T. Ohnishi, and M. Lippmaa
Institute for Solid State Physics, University of Tokyo, 515 Kashiwanoha, Chiba 2778581, Japan

(Received 11 September 2003; accepted 10 January 2004)

We have performed ferroelectric field effect experiments using an epitaxial heterostructure composed of ferroelectric $Pb(Zr_{0.2}Ti_{0.8})O_3$ and superconducting Nb-doped $SrTiO_3$. The films were prepared on (001) $SrTiO_3$ substrates by off-axis radio-frequency magnetron sputtering and pulsed-laser deposition. By switching the polarization field of the 500-Å-thick $Pb(Zr_{0.2}Ti_{0.8})O_3$ layer, a large change of about 30% in resistivity and a 20% shift of T_c ($\Delta T_c \sim 0.05$ K) were induced in the 400-Å-thick epitaxial Nb-doped $SrTiO_3$ layer. The relationship between T_c and the electrostatically modulated average carrier concentration can be mapped onto the phase diagram of chemically doped $SrTiO_3$. © *2004 American Institute of Physics.* [DOI: 10.1063/1.1667279]

Field effect in correlated oxide systems has recently been the subject of many studies.[1] So far, most of the investigations have been focused on high T_c oxide superconductors[2,3] and manganites.[4,5] Among perovskite oxides, electron doped $SrTiO_3$ (STO), e.g., $SrTiO_{3-x}$ and Nb-doped $SrTiO_3$ (Nb-STO), display superconductivity for carrier concentrations between about 1×10^{19} and 10^{21} cm^{-3}.[6–8] The critical temperature T_c depends on the carrier concentration and reaches a maximum of 0.3–0.4 K for a carrier concentration of about 1×10^{20} cm^{-3}. In spite of its low T_c, doped STO, being a very low carrier concentration superconductor, seems to be an ideal model system to exploit the potential demonstrated in recent conventional field effect experiments[2,9,10] and ferroelectric field effect experiments.[3,11] Although several previous reports have demonstrated field effect modulation of the STO normal state properties,[12–14] electrostatic modulation of superconductivity has not been achieved so far in this particular system. Another interesting aspect of STO is its simple cubic perovskite structure that should facilitate the realization of high quality thin films with flat surfaces. Furthermore, $Pb(Zr,Ti)O_3$ films, used as the ferroelectric gate oxide in ferroelectric field effect experiments,[3,11] have already been epitaxially fabricated on STO single crystal substrates with very smooth surfaces,[15] advantageous in developing the local ferroelectric field effect approach proposed by Ahn *et al.*[16] This latter approach may be a way to realize nanoscale superconducting switches, artificial Josephson junctions arrays, or re-writable pinning sites. Finally, the behavior of T_c as a function of carrier concentration in doped STO is different from that of conventional low carrier superconductors for which T_c increases monotonically with the carrier concentration.[17] In STO, T_c first increases with the carrier concentration n then, for n larger than 1×10^{20} cm^{-3}, T_c goes down, with superconductivity vanishing around 1×10^{21} cm^{-3}. It is generally accepted that this behavior can be explained by the plasmon and polar optic phonon model.[18] However, because the crystal quality in general gets worse as the carrier concentration increases (at high chemical doping), one could argue that the crystal quality has an influence on the T_c behavior. From this view point, field effect ''doping,'' which does not affect the crystal quality, is also of interest.

Epitaxial heterostructures composed of 500-Å-thick $Pb(Zr_{0.2}Ti_{0.8})O_3$ (PZT) and 400-Å-thick Nb-STO were fabricated on (001) STO single crystal substrates. For depositing the Nb-STO layer, a pulsed laser deposition method employing KrF excimer laser pulses (100 mJ) focused on a commercial 0.5 wt% Nb doped $SrTiO_3$ single crystal target was used. During deposition, the substrate temperature was kept at 1200 °C and the oxygen pressure at 2×10^{-7} Torr. As reported by Leitner *et al.*,[19] we found that the electronic properties of the Nb-STO films were strongly dependent on growth conditions. In order to get conductive films, high substrate temperature and low oxygen pressure during the deposition turned out to be necessary. With these extreme growth conditions, the mobility of our best films at low temperatures was ~300 $cm^2\,V^{-1}\,s^{-1}$, the largest value reported for thin films. We found, however, that even in the best films the carrier concentration, determined from Hall effect measurements, was $\sim3\times10^{19}$ cm^{-3}, which is only 20% of what is expected from the nominal Nb concentration. The ratio between the Nb doping and the active Nb donors is found to be less than previously reported (~50%) for thin films[19] and single crystals.[20,21] Clearly, although the STO films described in the following are of high quality, a complex process which will require further investigation controls the fraction of active Nb donors. By monitoring the intensity of reflection high-energy electron diffraction during the deposition, step-flow type growth[22] was observed. Atomic force microscopy (AFM) topographic images taken before the deposition of the PZT layer are consistent with this particular growth mode. Figure 1(a) shows the surface of a 400-Å-thick Nb-STO film. The image shows 4 Å high perovskite unit cell steps. No particles were observed even in large areas (typically 5×5 μm^2), a clear advantage for the subsequent growth of high quality epitaxial PZT. After deposition, the

[a]Electronic mail: kei.takahashi@physics.unige.ch

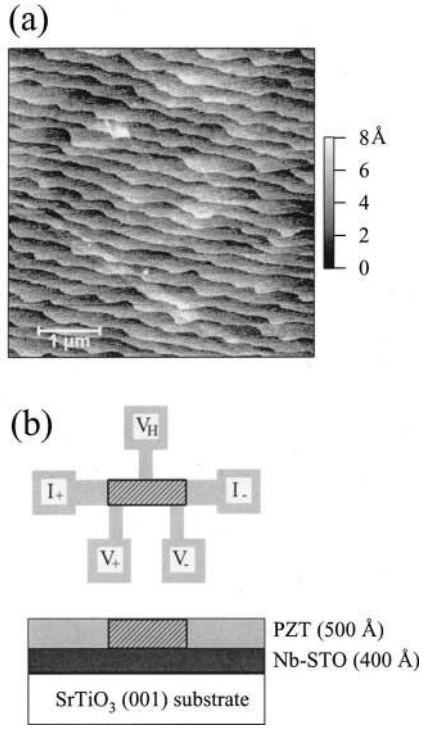

FIG. 1. (a) AFM image of a Nb-STO film, 400 Å thick, measured before the deposition of the PZT layer (5×5 μm). (b) Schematic top view and cross section of the field effect device. The dimensions of the fabricated transport paths are 40 μm (width) and 100 μm (length). The ferroelectric polarization was switched in the shaded area using an AFM.

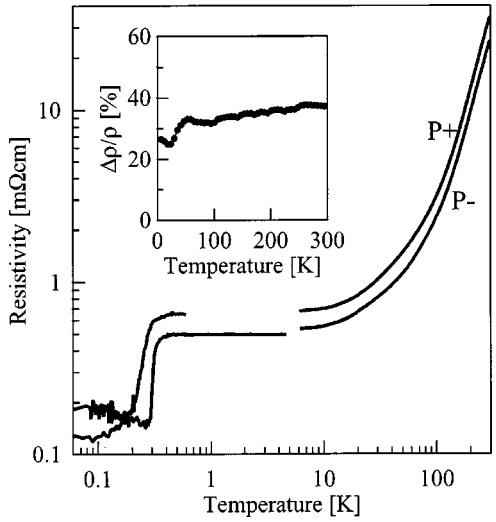

FIG. 2. (a) Temperature dependence of the resistivity for the two polarization states. $P+$ corresponds to the polarization direction that removes electrons from the Nb-STO layer. In the $P-$ state, the polarization field adds electrons to the film. The inset shows the temperature dependence of the resistivity difference ratio between the two polarization states defined as $\Delta\rho/\rho = [\rho(P+)-\rho(P-)]/\rho(P-)$.

films were cooled in 760 Torr of oxygen to avoid reducing the film and the substrate. The PZT layers were deposited by off-axis radio frequency magnetron sputtering in an argon–oxygen flow ($Ar:O_2=3:1$) at a total pressure of 0.18 Torr and at a substrate temperature of ~500 °C.[15] From x-ray diffraction analyses of these bilayers, the PZT layers are found to be c-axis oriented and single crystal like. However, no peaks of the Nb-STO layers could be identified because the Nb-STO lattice constant (for such low Nb doping) is almost identical to the one of the STO substrate. The film peaks are thus hidden by the intense substrate peaks. As schematically illustrated in Fig. 1(b), standard photolithography and ion-milling processes were used to pattern the devices in a geometry suitable for transport measurements. Measurements below 4.2 K and down to 50 mK were performed using a dilution refrigerator. To switch the direction of the ferroelectric polarization (parallel or antiparallel to the c axis), the metallic tip of an AFM was used as a mobile gate electrode, scanning at room temperature over the whole area of the conducting path [the shaded region shown in Fig. 1(b)]. During the scan, a constant voltage of +12 or −12 V was applied between the tip and the Nb-STO layer. During the transport measurements, there was no application of any gate voltage, making the device insensitive to possible leakage currents.

Figure 2 shows the temperature dependence of the resistivity, calculated using the Nb-STO thickness, for the two polarization states. The $P+$ state, poled using −12 V (on the tip), corresponds to the polarization direction which removes electrons from the Nb-STO layer. The $P-$ state poled using +12 V corresponds to the polarization state which adds electrons to the Nb-STO layer, effectively increasing the doping level. As can be seen, both states display metallic behavior. In the whole temperature range, large differences in the resistivities between the $P+$ and $P-$ states were observed. As expected from the electron character of doped STO, the resistivity of the $P-$ state is lower, in agreement with a field effect modulation of the electron carrier. The inset of Fig. 2 shows the resistivity (ρ) difference ratio between the two states defined as $(\Delta\rho/\rho = [\rho(P+)-\rho(P-)]/\rho(P-))$. Using a free electron model, a relationship between the changes in resistivity and carrier concentration (n) can be obtained: $\Delta\rho/\rho = -\Delta n\cdot\lambda/(n\cdot d+\Delta n\cdot\lambda/2)$, where d is the film thickness (400 Å), λ is the electrostatic screening length over which a carrier concentration profile is induced at the interface, and Δn is the average change in carrier concentration (over λ). $\Delta n\cdot\lambda$ being equal to $\Delta P/e$ where ΔP is the change in polarization, using $\Delta\rho/\rho \sim 30\%$ (see inset of Fig. 2) and $n\sim 3\times 10^{19}$ cm^{-3} (from Hall effect measurement), allows us to estimate ΔP to be ~6 μC/cm^2.[23,24] This ferroelectric polarization value is significantly lower than that observed in general for PZT[26] and lower than the one observed in other ferroelectric field effect devices.[11] Although not completely clear, the reason for this low polarization may be related to the difficulty in poling the PZT layer.[26] This problem may be due to inhomogeneities in the Nb-STO layer (possibly local changes in the electronic properties or a gradient of the properties as a function of thickness) or to a nonoptimal growth of the PZT layer. At low temperatures (below 1 K), sufficiently low measuring current was chosen to ensure an ohmic regime. Around 0.3 K, the resistivity of both polarization states drops abruptly, indicative of the transition to the superconducting state. Below the transition and down to 50 mK, the resistivity, however, does not reach zero but stays constant at a value of about 0.1 mΩ cm. This nonzero resistivity was also observed in Nb-STO single layer films, which implies that this nonzero residual resistivity is not due to the polarization field of the PZT layer but, most probably, to electronic inhomogeneities of the Nb-STO layer leading to

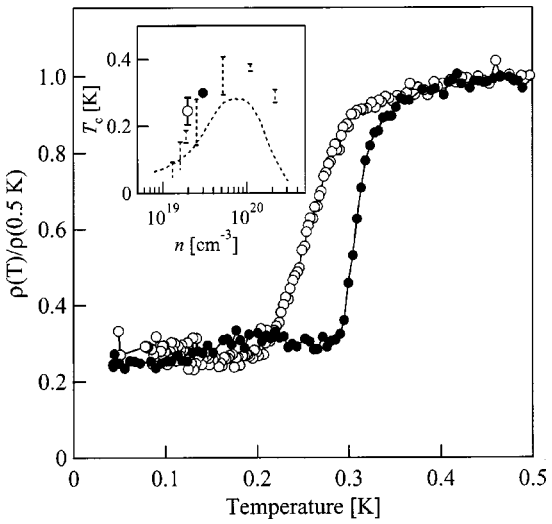

FIG. 3. Temperature dependence of the resistivity normalized at 0.5 K for the $P+$ state (○) and the $P-$ state (●). The inset shows the dependence of the critical temperature on carrier concentration for each polarization state. The behavior of reduced STO bulk crystals (dotted curve) and Nb doped STO bulk crystals (dotted bar) are also included.

nonsuperconducting regions cutting the superconducting current path. Preliminary measurements in magnetic fields applied perpendicular to the film plane showed that the superconducting transition was progressively suppressed and that, above 0.1 T, the normal metallic phase was observed down to the lowest accessible temperatures (50 mK).

Figure 3 shows the normalized resistivity at 0.5 K as a function of temperature for the $P+$ and $P-$ states. Upon polarization reversal a clear shift of T_c was observed. With T_c defined as the temperature at which the resistivity decreases to 50% of its value at 0.5 K, the T_c value for the $P-$ state is 0.30 K and that of the $P+$ state is 0.25 K. The change of polarization not only induces a shift of T_c but also modifies the transition width. As can be seen in Fig. 3, the $P+$ state transition is broader than the one of the $P-$ state. This broadening may reflect fluctuations related to the low superfluid density or intrinsic inhomogeneities as proposed in the case of underdoped high T_c superconductors.[27] Here, because of the uncertainties about the polarization of the PZT layer as well as possible inhomogeneities in the Nb-STO layer, more measurements will be necessary to test whether this broadening reflects the physics of the STO system or material imperfections. Finally, the inset of Fig. 3 shows the carrier concentration dependence of T_c for the $P+$ state and the $P-$ state and that for reduced and Nb doped STO bulk crystals.[7,8] Since the coherence length of superconducting STO is much larger than d,[28] although the change in carrier concentration is induced over a distance λ, the Cooper pairs experience an average effective interaction through the proximity effect.[29] We thus used the average carrier concentrations in the inset of Fig. 3. The carrier concentration of the $P-$ state ($\sim 3\times 10^{19}$ cm^{-3}), determined from Hall effect experiment at 20 K, is located in the underdoped region of the phase diagram (lower than 1×10^{20} cm^{-3}). That of $P+$ state is deduced as $\sim 2\times 10^{19}$ cm^{-3} from $\Delta n = \Delta P/e\cdot\lambda$. This is consistent with the fact that increasing the carrier concentration increases T_c. Even if there are slight deviations from the bulk crystal data, the electrostatic average doping can be rather well mapped onto the chemical doping phase diagram.

In conclusion, we have fabricated epitaxial heterostructures composed of PZT and Nb-STO on STO substrates. By switching the ferroelectric polarization field of the PZT layer, using the metallic tip of an AFM as a mobile gate electrode, a large temperature-independent relative change in the resistivity and a shift of T_c were observed. The relationship between T_c and the average carrier concentration for each polarization state fits with the phase diagram of chemically doped STO bulk crystals.

The authors would like to thank Patrycja Paruch for a careful reading of the manuscript. This work was supported by the Swiss National Science Foundation through the National Center of Competence in Research, "Materials with Novel Electronic Properties, MaNEP" and division II, New Energy and Industrial Technology Development Organization (NEDO) of Japan, and ESF (Thiox).

[1] See, for instance, the recent review by C. H. Ahn, J.-M. Triscone, and J. Mannhart, Nature (London) **424**, 1015 (2003).
[2] J. Mannhart, Supercond. Sci. Technol. **9**, 49 (1996).
[3] C. H. Ahn, S. Gariglio, P. Paruch, T. Tybell, L. Antognazza, and J.-M. Triscone, Science **284**, 1152 (1999).
[4] S. Mathews, R. Ramesh, T. Venkatesan, and J. Benedetto, Science **276**, 238 (1997).
[5] X. Hong, A. Posadas, A. Lin, and C. H. Ahn, Phys. Rev. B **68**, 134415 (2003).
[6] J. F. Schooley, W. R. Hosler, and M. L. Cohen, Phys. Rev. Lett. **12**, 474 (1964).
[7] E. R. Pfeiffer and J. F. Schooley, Phys. Lett. **29A**, 589 (1969).
[8] C. S. Koonce, M. L. Cohen, J. F. Schooley, W. R. Hosler, and E. R. Pfeiffer, Phys. Rev. **163**, 380 (1967).
[9] V. V. Lemanov and A. L. Kholkin, Phys. Solid State **36**, 841 (1994).
[10] D. Matthey, S. Gariglio, and J.-M. Triscone, Appl. Phys. Lett. **83**, 3758 (2003).
[11] S. Gariglio, C. H. Ahn, D. Matthey, and J.-M. Triscone, Phys. Rev. Lett. **88**, 067002 (2002).
[12] I. Pallecchi, G. Grassano, D. Marré, L. Pellegrino, M. Putti, and A. S. Siri, Appl. Phys. Lett. **78**, 2244 (2001).
[13] D. Marré, A. Tumino, E. Bellingeri, I. Pallecchi, L. Pellegrino, and A. S. Siri, J. Phys. D **36**, 896 (2003).
[14] K. Ueno, I. H. Inoue, H. Akoh, M. Kawasaki, Y. Tokura, and H. Takagi, Appl. Phys. Lett. **83**, 1755 (2003).
[15] T. Tybell, C. H. Ahn, and J.-M. Triscone, Appl. Phys. Lett. **75**, 856 (1999).
[16] C. H. Ahn, T. Tybell, L. Antognazza, K. Char, R. H. Hammond, M. R. Beasley, Ø. Fischer, and J.-M. Triscone, Science **276**, 1100 (1997).
[17] J. K. Hulm, M. Ashkin, D. W. Deis, and C. K. Jones, Prog. Low Temp. Phys. **6**, 205 (1970).
[18] Y. Takada, J. Phys. Soc. Jpn. **49**, 1267 (1980).
[19] A. Leitner, C. T. Rogers, J. C. Price, D. A. Rudman, and D. R. Herman, Appl. Phys. Lett. **72**, 3065 (1998).
[20] H. P. R. Frederikse and W. R. Hosler, Phys. Rev. **161**, 822 (1967).
[21] C. Lee, J. Destry, and J. L. Brebner, Phys. Rev. B **11**, 2299 (1975).
[22] M. Lippmaa, N. Nakagawa, M. Kawasaki, S. Ohashi, and H. Koinuma, Appl. Phys. Lett. **76**, 2439 (2000).
[23] We notice that the mobility in STO depends on the carrier density at low temperatures (Ref. 25). The free electron formula used has thus to be taken with care.
[24] O. N. Tufte and P. W. Chapman, Phys. Rev. **155**, 796 (1967).
[25] B. Jaffe, W. R. Cook, and H. Jaffe, *Piezoelectric ceramics*. (Academic, London, 1971).
[26] We have noticed that repeated AFM poling of the same area improved the size of the ferroelectric field effect, suggesting incomplete poling of the PZT layer.
[27] See, for instance, V. J. Emery and S. A. Kivelson, Nature (London) **374**, 434 (1995), Phys. Rev. Lett. **74**, 3253, (1995).
[28] A. Leitner, D. Olaya, C. T. Rogers, and J. C. Price, Phys. Rev. B **62**, 1408 (2000).
[29] G. Deutscher and P. G. de Gennes, *Superconductivity*, edited by P. D. Parks (Dekker, New York, 1969), p. 1005.